arXiv:1703.00685v1 [hep-ph] 2 Mar 2017

A Radiative Neutrino Model Linking to A Monochromatic Gamma-ray Line

Seungwon Baek,[1,*] Hiroshi Okada,[2,†] and Yuta Orikasa[3,‡]

[1] *School of Physics, KIAS, Seoul 130-722, Korea*

[2] *Physics Division, National Center for Theoretical Sciences, Hsinchu, Taiwan 300*

[3] *Institute of Experimental and Applied Physics, Czech Technical University, Prague 12800, Czech Republic*

(Dated: December 14, 2024)

Abstract

We explore the possibility to explain the monochromatic Fermi-LAT anomaly at 42.7 GeV dark matter mass in the framework of radiatively induced neutrino mass model at two level. Here we prepare the Zee-Babu type scenario with Z_3 discrete symmetry, in which we consider the neutrino oscillation data, lepton flavor violations, and bosonic dark matter candidate. A $\mu - e$ conversion rate, which can be tested in the near future experiment such as PRISM/PRIME, is estimated and its allowed range is shown through the global analysis.

Keywords:

*Electronic address: swbaek@kias.re.kr

†Electronic address: macokada3hiroshi@cts.nthu.edu.tw

‡Electronic address: Yuta.Orikasa@utef.cvut.cz

	Lepton Fields			Scalar Fields		
	L_L	e_R	$N_{L/R}$	Φ	η	χ
$SU(2)_L$	**2**	**1**	**1**	**2**	**2**	**1**
$U(1)_Y$	$-\frac{1}{2}$	-1	0	$\frac{1}{2}$	$\frac{1}{2}$	0
Z_3	1	1	ω	1	ω	ω

TABLE I: Contents of fermion and scalar fields and their charge assignments under $SU(2)_L \times U(1)_Y \times Z_3$.

I. INTRODUCTION

Radiatively induced neutrino masses could be one of the promising scenarios to make a strong correlation between neutrinos and any fields that are introduced inside the loop. If one wants to introduce a dark matter (DM) candidate in one's model, its testability is enhanced due to the fact that the parameter space is strongly constrained by neutrino data. Especially two-loop induced models that we will focus on in this paper are widely studied in various aspects [1–34].

A smoking-gun signal for dark matter is monochromatic gamma ray. In this letter, we explain a possible anomaly of monochromatic photon at 42.7 GeV which can be explained by annihilating DM with cross section, 5×10^{-28} cm$^3/s$ (BF/1000)$^{-1}$, BF being boost factor [35], in the framework of Zee-Babu type of neutrino model. We estimate the lepton flavor violating (LFV) $\mu - e$ conversion rate in *Titanium* nuclei that will be tested in the near future experiment such as PRISM/PRIME [36] as well as muon anomalous magnetic moment.

This paper is organized as follows. In Sec. II, we show our model, including neutrino sector, LFVs, muon anomalous magnetic moment. In Sec. III, we analyze bosonic DM candidate to explain relic density and direct detection. In Sec. IV, we present the results of numerical analysis. We conclude and discuss in Sec. V.

II. MODEL SETUP

In this section, we introduce our model. We introduce a global Z_3 symmetry in addition to the SM gauge symmetry. The particle contents and their charges under $SU(2)_L \times U(1)_Y \times Z_3$

are shown in Tab. I. We add three family of iso-spin singlet vector-like neutral fermions N[1], an iso-spin doublet scalar η, and an isospin singlet scalar χ to the SM fiels. Due to Z_3 symmetry, only the SM-like Higgs Φ, has vacuum expectation value (VEV), $\langle \Phi^0 \rangle = v/\sqrt{2}$ [21]. All the new particles, N, η and χ are charged under Z_3 with the same charge, ω.

Then the relevant Lagrangian and Higgs potential under these symmetries are given by

$$
\begin{aligned}
-\mathcal{L}_Y &= (y_\ell)_{ij} \bar{L}_{L_i} \Phi e_{R_j} + (y_\eta)_{ij} \bar{L}_{L_i} (i\sigma_2) \eta^* N_{R_j} + y_{N_{R_{ij}}} \bar{N}^c_{R_i} N_{R_j} \chi + y_{N_{L_{ij}}} \bar{N}^c_{L_i} N_{L_j} \chi + M_{N_{ij}} \bar{N}_{L_i} N_{R_j} + \text{h.c.}, \\
\mathcal{V} &= m_\Phi^2 \Phi^\dagger \Phi + m_\eta^2 |\eta|^2 + m_\chi^2 |\chi|^2 + \mu_{\eta\chi} (\Phi^\dagger \eta \chi^* + \text{h.c.}) + \mu_\chi (\chi^3 + \text{h.c.}) + \lambda_\Phi (\Phi^\dagger \Phi)^2 \\
&\quad + \lambda_0 (\Phi^\dagger \eta \chi^2 + \text{h.c.}) + \lambda_\eta (\eta^\dagger \eta)^2 + \lambda_\chi (\chi^* \chi)^2 + \lambda_{\Phi\eta} (\Phi^\dagger \Phi)(\eta^\dagger \eta) + \lambda'_{\Phi\eta} |\Phi^\dagger \eta|^2 \\
&\quad + \lambda_{\Phi\chi} (\Phi^\dagger \Phi) \chi^* \chi + \lambda_{\eta\chi} (\eta^\dagger \eta) \chi^* \chi,
\end{aligned}
\tag{II.1}
$$

where σ_2 is the second Pauli matrix, $i, j = 1 - 3$, ~~$\sigma_i (i = 1 - 3)$~~ is Pauli matrix, and the first term of $\mathcal{L}_Y$ can generate the SM charged-lepton masses $m_\ell \equiv y_\ell v/\sqrt{2}$ after Φ obtains VEV. We assume the N_i's are the mass eigenstates, *i.e.*, $M_{N_{ij}} = M_{N_i} \delta_{ij}$. We work in the basis where all the coefficients are real and positive for simplicity. The scalar fields can be parameterized in the unitary gauge as follows:

$$
\Phi = \begin{bmatrix} 0 \\ \frac{v+\phi}{\sqrt{2}} \end{bmatrix}, \quad \eta = \begin{bmatrix} \eta^+ \\ \eta \end{bmatrix}, \quad \chi,
\tag{II.2}
$$

where η and χ are complex inert bosons, $v \simeq 246$ GeV is VEV of the Higgs doublet, and ϕ is the SM Higgs boson and with mass $m_\phi \approx 125.5$ GeV.

Notice here that we have mixing between inert bosons, the resulting mass eigenvalues M_H, and rotation matrix being respectively given as

$$
O_H^T M_H O_H = \begin{bmatrix} m_{H_1} & 0 \\ 0 & m_{H_2} \end{bmatrix}, \quad \begin{bmatrix} \chi \\ \eta \end{bmatrix} = O \begin{bmatrix} H_1 \\ H_2 \end{bmatrix} = \begin{bmatrix} \cos\alpha & \sin\alpha \\ -\sin\alpha & \cos\alpha \end{bmatrix} \begin{bmatrix} H_1 \\ H_2 \end{bmatrix},
\tag{II.3}
$$

where $H_{1(2)}$ and α are written in terms of Higgs potential, and we use the short hand notation $s_\alpha (c_\alpha)$ for $\sin\alpha (\cos\alpha)$ below [2].

[1] The N_R's are introduced to give masses to N's.
[2] See ref. [21] for details.

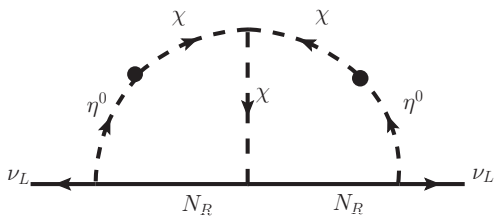

FIG. 1: The two-loop diagram the generation of neutrino masses. The blobs indicate the scalar mixing between η^0 and χ.

A. Neutrino masses

The active neutrino mass matrix m_ν is generated at two-loop level as shown in Figure 1, and its formula is given by

$$(m_\nu)_{ij} = \frac{12\sqrt{2}\mu_\chi s_\alpha^2 c_\alpha^2 (y_\eta)_{ia}(y_N)_{ab}(y_\eta)^T_{bj}}{(4\pi)^4} F_{II} \equiv (y_\eta)_{ia}(y'_N)_{ab}(y_\eta)^T_{bj}, \tag{II.4}$$

$$F_{II} = \int \frac{[dx]}{z-1}\int [da]\left[c_\alpha^2\left[\ln\left(\frac{\Delta_{111}}{\Delta_{112}}\right) - \ln\left(\frac{\Delta_{211}}{\Delta_{212}}\right)\right] + s_\alpha^2\left[\ln\left(\frac{\Delta_{222}}{\Delta_{221}}\right) - \ln\left(\frac{\Delta_{122}}{\Delta_{121}}\right)\right]\right], \tag{II.5}$$

$$\Delta_{\ell mn} = -a\frac{xM^2_{N_b} + ym^2_{H_n} + zm^2_{H_m}}{z^2 - z} + bM^2_{N_a} + cm^2_{H_\ell}, \tag{II.6}$$

where $[dx] \equiv dxdydz\delta(x+y+z-1)$, $[da] \equiv dadbdc\delta(a+b+c-1)$, and we assume $y_N \equiv y_{N_R} \approx y_{N_L}$.

The active neutrino mass matrix, $(m_\nu)_{ij}$, can be generally diagonalized by the Pontecorvo-Maki-Nakagawa-Sakata (PMNS) mixing matrix $V_{\rm MNS}$ [38] as

$$(m_\nu)_{ij} = (V^*_{\rm MNS} D_\nu V^\dagger_{\rm MNS})_{ij}, \quad D_\nu \equiv (0, m_{\nu_2}, m_{\nu_3}), \tag{II.7}$$

$$V_{\rm MNS} = \begin{bmatrix} c_{13}c_{12} & c_{13}s_{12} & s_{13}e^{-i\delta} \\ -c_{23}s_{12} - s_{23}s_{13}c_{12}e^{i\delta} & c_{23}c_{12} - s_{23}s_{13}s_{12}e^{i\delta} & s_{23}c_{13} \\ s_{23}s_{12} - c_{23}s_{13}c_{12}e^{i\delta} & -s_{23}c_{12} - c_{23}s_{13}s_{12}e^{i\delta} & c_{23}c_{13} \end{bmatrix}, \tag{II.8}$$

where we assume one of three neutrino masses is zero with normal ordering, neglect the Majorana phase, and fix the Dirac phase $\delta = -\pi/2$ in the numerical analysis for simplicity.

Then we apply the generalized Casas-Ibarra parametrization [3] to our analysis, where we use the observed neutrino oscillation with global fit [40]. Then Yukawa coupling y_η can be

[3] In our case, the central matrix is not diagonal but the symmetric matrix which is proportional to y_N.

rewritten in terms of the following parameters:

$$y_\eta \approx V^*_{\rm MNS}\sqrt{D_\nu}\mathcal{O}(\theta_{1,2,3})\left({y_N}'^{Ch}\right)^{-1}, \tag{II.9}$$

where $\mathcal{O}(\theta_{1,2,3})$ is an arbitrary 3×3 orthogonal matrix with three complex values $\theta_{1,2,3}$,

and $y_N'^{Ch}$ is Cholesky decomposed matrix. This matrix is a lower triangular matrix and satisfies the following relation (see appendix A),

$$y'_N = y_N'^{Ch}\left(y_N'^{Ch}\right)^T. \tag{II.10}$$

Lepton flavor violations(LFVs) arises from the term y_η at one-loop level [4], and its form is given by

$$\mathrm{BR}(\ell_i\to\ell_j\gamma) = \frac{48\pi^3 C_{ij}\alpha_{\rm em}}{\mathrm{G_F^2}}\left(|a_{R_{ij}}|^2+\epsilon_{ij}|a_{L_{ij}}|^2\right), \tag{II.11}$$

$$a_{R_{ij}} = a_{L_{ij}} = \sum_{k=1,2,3}\frac{(y_\eta)_{jk}(y_\eta^\dagger)_{ki}}{(4\pi)^2}F_{lfv}(M_{N_k},m_{\eta^\pm}), \tag{II.12}$$

$$F_{lfv}(m_a,m_b) = \frac{2m_a^6+3m_a^4m_b^2-6m_a^2m_b^4+6m_b^6+12m_a^4m_b^2\ln(m_b/m_a)}{12(m_a^2-m_b^2)^4}, \tag{II.13}$$

where $\epsilon_{ij}\equiv(m_{\ell_j}/m_{\ell_i})^2(\ll 1)$, $\eta^\pm$ is the singly charged component of η, $\mathrm{G_F}\approx 1.17\times 10^{-5}[\mathrm{GeV}]^{-2}$ is the Fermi constant, $\alpha_{\rm em}\approx 1/137$ is the fine structure constant, $C_{21}\approx 1$, $C_{31}\approx 0.1784$, and $C_{32}\approx 0.1736$. Experimental upper bounds are respectively given by $\mathrm{BR}(\mu\to e\gamma)\lesssim 4.2\times 10^{-13}$, $\mathrm{BR}(\tau\to e\gamma)\lesssim 3.3\times 10^{-8}$, and $\mathrm{BR}(\tau\to\mu\gamma)\lesssim 4.4\times 10^{-8}$.
The $\mu-e$ *conversion* is obtained by using $a_{R/L}$, and its capture rate R is approximately given by [5]

$$R\approx\frac{C_{\mu e}|Z|^2}{\Gamma_{\rm cap}}\left(|a_{R_{ij}}|^2+\epsilon_{ij}|a_{L_{ij}}|^2\right),\quad C_{\mu e}\approx 4\alpha_{\rm em}^5\frac{Z_{\rm eff}^4|F(q)|^2m_\mu^5}{Z}, \tag{II.14}$$

where Z, $Z_{\rm eff}$, $F(q)$, and R are given in table II.

Here let us define $Y\equiv\frac{R}{\mathrm{BR}(\mu\to e\gamma)}$, since their flavor structures are same. Then it is given by

$$Y\approx 1.22\times 10^{-24}\left(\frac{ZZ_{\rm eff}^4|F(q)|^2}{\Gamma_{\rm cap}}\right). \tag{II.15}$$

[4] Recently sophisticated analysis has been don by ref. [39]
[5] We neglect the contribution to the Z-penguin diagram due to suppression factor $(m_\ell/M_N)^2$.

Nucleus ${}^{A}_{Z}N$	$Z_{\rm eff}$	$\lvert F(-m_\mu^2)\rvert$	$\lvert\Gamma_{\rm capt}(10^6{\rm sec}^{-1})$	Experimental bound (Future bound)	$Y \equiv \frac{R}{{\rm BR}(\mu\to e\gamma)}$
${}^{27}_{13}Al$	11.5	0.64	0.7054	$(R_{Al} \lesssim 10^{-16})$ [41]	0.25
${}^{48}_{22}Ti$	17.6	0.54	2.59	$R_{Ti} \lesssim 4.3\times10^{-12}$ [42] ($\lesssim 10^{-18}$ [36])	0.44
${}^{197}_{79}Au$	33.5	0.16	13.07	$R_{Au} \lesssim 7\times10^{-13}$ [43]	0.36
${}^{208}_{82}Pb$	34	0.15	13.45	$R_{Pb} \lesssim 4.6\times10^{-11}$ [44]	0.34

TABLE II: Summary for the the μ-e conversion in various nuclei: Z, $Z_{\rm eff}$, $F(q)$, $\Gamma_{\rm capt}$, and the bounds on the capture rate R.

Depending on the nuclei, $Y \approx \mathcal{O}(0.1)$, as is listed in table II. It suggests that each constraint of the $\mu - e$ conversion is always satisfied once we satisfy the constraint of $\mu \to e\gamma$. We will discuss the sensitivity of future experiments, R_{Ti} and R_{Al}, in the numerical analysis.

New contributions to the muon anomalous magnetic moment (muon $g-2$) is always negative, which is not consistent with the current measurement at $\sim 3\sigma$ level, where the formula is given by $\Delta a_\mu \approx -m_\mu[a_{R_{\mu\mu}} + a_{L_{\mu\mu}}]$. The experimental value is about $\mathcal{O}(10^{-9})$.

III. DARK MATTER

Here we consider $H_1(\equiv X)$ as the dark matter(DM) candidate, which is a complex scalar. Since we consider the anomaly in the photon line-like signature at $M_X \approx 43$ GeV reported by Fermi-LAT experiment [35], allowed DM annihilation modes are kinematically restricted to $XX^{(*)} \to b\bar{b}, \ell\bar{\ell}, \nu\bar{\nu}$.

Relic density of DM: Here we discuss the relic density of DM. Annihilation channels to explain the relic density are $XX^{(*)} \to b\bar{b}, \ell\bar{\ell}, \nu\bar{\nu}$, and their cross sections are respectively

given by

$$\sigma v_{\rm rel} \approx \sum_{f=X^{(*)},b,\nu} \int_0^\pi \sin\theta d\theta \frac{|M(XX^* \to f\bar{f})|^2}{16\pi s} \sqrt{1-\frac{4m_f^2}{s}}, \tag{III.1}$$

$$|M(XX^* \to \nu_i \bar{\nu}_j)|^2 \approx s_\alpha^4 \left| \frac{(y_\eta)_{ia}(y_\eta^\dagger)_{aj}}{t-M_{N_a}^2} \right|^2 M_X^4 \sin^2\theta v_{\rm rel}^2 + 4C_Z^2 M_X^4 (A_{L\nu}^2 + A_{R\nu}^2) \sin^2\theta v_{\rm rel}^2$$
$$+ 4\frac{M_X^4 s_\theta^2 s_\alpha^2 A_{L\nu}(y_\eta)_{ia}(y_\eta^\dagger)_{aj} C_Z}{t-M_{N_a}^2} v_{\rm rel}^2, \tag{III.2}$$

$$|M(XX^* \to f\bar{f})|^2 \approx 2C_f M_X^2 \left[4C_\phi^2 + (C_\phi^2 + 2(A_{Lf}^2 + A_{Rf}^2) C_Z^2 \sin^2\theta M_X^2) v_{\rm rel}^2 \right], \tag{III.3}$$

$$C_\phi \equiv \frac{\mu_{2X\phi} m_f}{v(s-m_\phi^2)}, \quad C_Z \equiv \frac{g_2\sqrt{g_1^2+g_2^2}s_\alpha^2}{2c_{tw}(s-m_Z^2)}, \; A_{L\nu} = \frac{1}{2}, \; A_{L\ell} = -\frac{1}{2} + s_{tw}^2, \; A_{R\ell} = s_{tw}^2,$$
$$A_{Lu} = \frac{1}{2} - \frac{2}{3}s_{tw}^2, \; A_{Ru} = -\frac{2}{3}s_{tw}^2, \; A_{Ld} = -\frac{1}{2} + \frac{1}{3}s_{tw}^2, \; A_{Rd} = \frac{1}{3}s_{tw}^2, \tag{III.4}$$

where $C_f = 1$ for $f = \ell$ and $C_f = 3$ for $f = q$, $\mu_{2X\phi} \equiv c_\alpha^2 v\lambda_{\Phi\chi} + s_\alpha^2 v(\lambda_{\Phi\eta} + \lambda'_{\Phi\eta}) + \sqrt{2}c_\alpha s_\alpha \mu_{\eta\chi}$, $s \approx M_X^2(4+v_{\rm rel}^2)$ and $t \approx M_X^2(-1+m_f^2/M_X^2 + \sqrt{1-m_f^2/M_X^2}c_\theta v_{\rm rel} - v_{\rm rel}^2/2)$ are the Mandelstam variables.

If we take terms up to the $v_{\rm rel}^2$ in $v_{\rm rel}$ expansion for all the modes, $\sigma v_{\rm rel} \approx a_{\rm eff} + b_{\rm eff} v_{\rm rel}^2$, we finally obtain the relic density as [45]

$$\Omega h^2 \approx \frac{1.07 \times 10^9 x_f^2}{g_*^{1/2} M_{\rm pl}[{\rm GeV}] \left(a_{\rm eff} x_f + 3b_{\rm eff}\right)}, \tag{III.5}$$

where $g_* \approx 100$ is the total number of effective relativistic degrees of freedom at the time of freeze-out, $M_{\rm pl} = 1.22 \times 10^{19}$[GeV] is the Planck mass, $x_f \approx 25$, and $a_{\rm eff}$, and $b_{\rm eff}$ are coefficients in the $v_{\rm rel}^2$ expansion of the annihilation cross section. The observed relic density reported by Planck suggests that $\Omega h^2 \approx 0.12$ [46].

Notice here that C_Z^2(or equivalently s_α^4) and $\mu_{2X\phi}$ should be tiny enough in order to evade the direct detection searches at LUX [47].

IV. NUMERICAL ANALYSIS

For the numerical analysis in this section, we will fix some parameters; $(M_{N_1}, M_{N_2}, M_{N_3}) = (200, 300, 400)$ GeV and $(m_{H_1}, m_{H_2}) = (42.7, 550)$ GeV in order to simplify our numerical analysis. [6] Then the range of the other input parameters are randomly

[6] As a consequence, the value of the two-loop function F_{II} is fixed, otherwise it is too complicated to perform the numerical analysis.

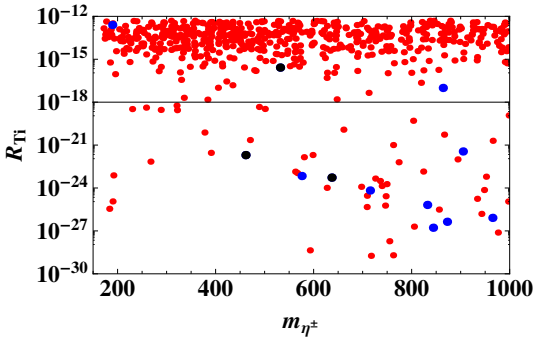

FIG. 2: Scatter plot of the *Titanium* capture rate R_{Ti} as a function the $\eta^\pm$ mass, where the red points are $|\Delta a_\mu| < 10^{-10}$, the blue ones are $10^{-10} \leq |\Delta a_\mu| < 10^{-9}$, and the black ones are $10^{-9} \leq |\Delta a_\mu|$. The horizontal black line represents the future upper bound on R_{Ti}.

selected by as follows:

$$(y_N)_{ij} \in [0,1],\ \theta_{1,2,3} \in [0, 2\pi) + i[0, 10^3),\ s_\alpha \in [0.001, 0.1], \tag{IV.1}$$

$$(\mu_\chi, \mu_{\eta\chi}) \in [10, 1000]\ \text{GeV},\ m_{\eta^\pm} \in [100, 1000]\ \text{GeV}, \tag{IV.2}$$

where y_N is symmetric matrix, $\theta_{1,2,3}$ are arbitrary complex values in the Casas-Ibarra parameters. Notice here y_η should satisfy the perturbative limit; $y_\eta \lesssim \sqrt{4\pi}$, and the upper value of s_α is taken to be 0.1 to suppress the spin independent DM-nucleon scattering cross section so that the direct detection search bounds from LUX or PandaX are satisfied as mentioned before. Among randomly chosen 10^7 points, we obtain 616 allowed points satisfying all the constraints discussed above. In fig. 2, we show a scatter plot of the *Titanium* capture rate R_{Ti} in terms of the $\eta^\pm$ mass, where the red points are $|\Delta a_\mu| < 10^{-10}$, the blue ones are $10^{-10} \leq |\Delta a_\mu| < 10^{-9}$, and the black ones are $10^{-9} \leq |\Delta a_\mu|$. [7] From the figure we can see that the typical allowed points predict $R_{Ti} \sim 10^{-15} - 10^{-13}$. And the upper bound 1.8×10^{-13} arises from the constraint of $\mu \to e\gamma$ rather than the constraint of R_{Ti} itself as discussed in the part of LFVs. But sometimes tiny values of R_{Ti} can be achieved and these can evade the future experiment sensitivity, $\sim 10^{-18}$, depicted by black horizontal line. Notice here that lighter mass range of $\eta^\pm$, 100 GeV $\lesssim m_{\eta^\pm} \lesssim$ 150 GeV, is forbidden by the LFVs.

[7] Notice here again that muon $g-2$ is always negative that is against the current experimental result at about 3σ level. However if negative value might be favored in near future experiments, it makes sense.

V. FERMI-LAT AT 42.7 GEV

The main mode to the 2 photon process at one-loop level arises from the point interaction $XX^*\eta^+\eta^-$. [8] The cross section is given by

$$(\sigma v)_{\rm FL} \approx \frac{|\lambda_\eta s_\alpha^2 + \lambda_{\eta\chi} c_\alpha^2|^2}{64\pi M_X^2} \int_0^\pi \sin\theta d\theta G^{\mu\nu}_{\eta^\pm}(G^*_{\mu\nu})_{\eta^\pm} \approx \frac{|\lambda_\eta s_\alpha^2 + \lambda_{\eta\chi} c_\alpha^2|^2}{32\pi M_X^2} G^{\mu\nu}_{\eta^\pm}(G^*_{\mu\nu})_{\eta^\pm}, \tag{V.1}$$

$$G^{\mu\nu}_{\eta^\pm} \approx -\frac{[g^{\mu\nu} k_1\cdot k_2 - k_1^\nu k_2^\mu]}{(4\pi)^2} \int dxdydz \frac{xy\delta(x+y+z-1)}{m^2_{\eta^\pm} - 2xyk_1\cdot k_2}, \tag{V.2}$$

$$G^{\mu\nu}_{\eta^\pm}(G^*_{\mu\nu})_{\eta^\pm} \approx \frac{8M_X^4}{(4\pi)^4}\left|\int dxdy \frac{xy}{m^2_{\eta^\pm} - 4xyM_X^2}\right|^2 = \frac{r^2}{32\pi^4}\left|\int_0^1 dx \int_0^{1-x} dy \frac{xy}{1-4xyr}\right|^2, \tag{V.3}$$

where we have used $k_1\cdot k_2 \approx 2M_X^2$ in the last equation, and $0 \lesssim r \equiv \frac{M_X^2}{m^2_{\eta^\pm}} \lesssim 1$. Adapting $M_X \approx 43$ GeV, the cross section to explain the Fermi-LAT anomaly at 43 GeV should be 5×10^{-28} cm$^3/s$ or equivalently 4.27×10^{-11} GeV^{-2} [35]. [9].

Here we assume $\lambda \equiv \lambda_\eta \approx \lambda_{\eta\chi}$ for simplicity, then one finds that $(\sigma v)_{\rm FL}$ is independent of α, and λ, and can be rewritten in term of experimental value and some parameters in Eq.(V.1) as

$$\lambda \approx \sqrt{\frac{4.27\times 10^{-11}}{\rm GeV^2}\frac{32\pi M_X^2}{G^{\mu\nu}_{\eta^\pm}(G^*_{\mu\nu})_{\eta^\pm}}}. \tag{V.4}$$

Notice here now that we have only two free parameters $m_{\eta^\pm}$ [10] and λ. Thus the Fermi-LAT anomaly is always satisfied whenever we use the above formula, where $\lambda \lesssim 4\pi$ should be satisfied arising from the perturbative limit. Furthermore one can analyze the Fermi-LAT anomaly independently, since λ does not contribute to the other phenomenologies that we discussed above. We show the allowed line to satisfy the Fermi-LAT anomaly at 42.7 GeV DM mass with $(\sigma v)_{\rm FL} \approx 5\times 10^{-28}$ cm$^3/s$ in terms of $m_{\eta^\pm}$ and λ In fig. 3, where we take the same input region as numerical analysis.

Since the typical scale of λ is 0.1, Fermi-LAT anomaly is always satisfied at this region, which is worth comparing to the case of the fermionic DM candidate [49]. Notice here that lighter mass region 100 GeV $\lesssim m_{\eta^\pm} \lesssim$ 150 GeV is ruled out from the LFV constraint.

[8] Notice here that the diagram with $W^\pm$ boson running inside the loop can be neglected in our framework because this mode is proportional to s_α^4. The detailed computation can be found in ref. [48].

[9] The ref.[49] discusses the Majorana fermionic DM case.

[10] Since $m_{\eta^\pm}$ contributes to the LFVs, too lighter mass is not in favored. In this sense, this mass is slightly restricted.

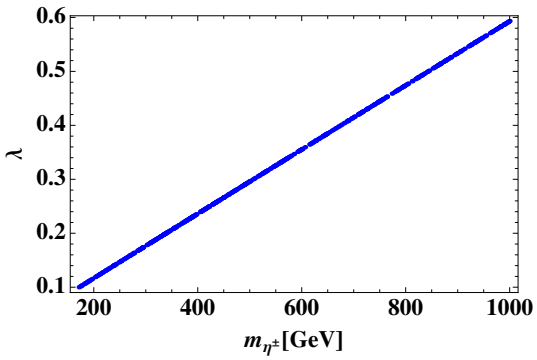

FIG. 3: The allowed line to satisfy the Fermi-LAT anomaly at 42.7 GeV DM mass with $(\sigma v)_{\rm FL} \approx 5 \times 10^{-28}$ cm$^3/s$ in terms of $m_{\eta^\pm}$ and λ, where we take 100 GeV $\leq m_{\eta^\pm} \leq$ 1000 GeV.

VI. SUMMARIES AND DISCUSSIONS

We have explored the possibility to explain the monochromatic Fermi-LAT anomaly at 42.7 GeV dark matter mass in the framework of radiatively induced neutrino mass model at two-loop level. Here we have prepared the Zee-Babu type scenario with Z_3 discrete symmetry, in which we have considered the neutrino oscillation data, lepton flavor violations, and bosonic dark matter candidate. Muon $g-2$ can be sizable but with negative sign, which conflicts with the current experimental data. Here we mention the way to get positive and sizable muon $g-2$.

The minimal way is to introduce the singly-charged boson h^+ with ω under Z_3 symmetry. Then h^+ and η^+ mix each other, and we have another source of muon $g-2$ that can explain the sizable positive deviation of muon $g-2$. It does not affect the neutrino sector, and this kind of scenario has already been discussed, for example, in ref. [50].

A $\mu-e$ conversion rate has also been estimated and found that the allowed points lies over the wide range, which can be tested in the near future experiment such as PRISM/PRIME. To explain the Fermi-LAT experiment at 42.7 GeV dark matter mass with 5×10^{-28} cm$^3/s$ of the non-relativistic cross section, we have used the simplest interaction, therefore, point-like interaction at one-loop level via $\eta^\pm$. We have shown the allowed line, in which order $\mathcal{O}(0.1)$ quartic coupling is enough to explain it that is worthwhile to compare to the case of the fermionic DM candidate.

As another aspect, since DM has nonzero charge under the Z_3 symmetry, it has self-

interacting modes that can play an crucial role in relaxing or resolving the dwarf problem around the earth. This topic have already been discussed in several refs. [51].

Acknowledgments

H. O. is sincerely grateful for all the KIAS members in Korea. This work is supported in part by National Research Foundation of Korea (NRF) Research Grant NRF-2015R1A2A1A05001869 (SB).

Appendix A: Cholesky decomposition

A symmetric matrix M is factorized by Cholesky decomposition. The decomposition is as follows;

$$M = \begin{bmatrix} m_{11} & m_{12} & m_{13} \\ m_{12} & m_{22} & m_{23} \\ m_{13} & m_{23} & m_{33} \end{bmatrix} = LL^T, \tag{A.1}$$

where L is a lower triangular matrix. The explicit form for the matrix L is

$$L = \begin{bmatrix} l_{11} & 0 & 0 \\ l_{21} & l_{22} & 0 \\ l_{31} & l_{32} & l_{33} \end{bmatrix}, \tag{A.2}$$

$$l_{11} = \pm\sqrt{m_{11}}, \tag{A.3}$$

$$l_{21} = \frac{m_{12}}{l_{11}}, \tag{A.4}$$

$$l_{22} = \pm\sqrt{m_{22} - l_{21}^2}, \tag{A.5}$$

$$l_{31} = \frac{m_{13}}{l_{11}}, \tag{A.6}$$

$$l_{32} = \frac{m_{32} - l_{31}l_{21}}{l_{22}}, \tag{A.7}$$

$$l_{33} = \pm\sqrt{m_{33} - l_{31}^2 - l_{32}^2}. \tag{A.8}$$

We use all positive case.

---

[1] A. Zee, Nucl. Phys. B **264**, 99 (1986); K. S. Babu, Phys. Lett. B **203**, 132 (1988).

[2] K. S. Babu and C. Macesanu, Phys. Rev. D **67**, 073010 (2003) [hep-ph/0212058].

[3] D. Aristizabal Sierra and M. Hirsch, JHEP **0612**, 052 (2006) [hep-ph/0609307].

[4] M. Nebot, J. F. Oliver, D. Palao and A. Santamaria, Phys. Rev. D **77**, 093013 (2008) [arXiv:0711.0483 [hep-ph]].

[5] D. Schmidt, T. Schwetz and H. Zhang, Nucl. Phys. B **885**, 524 (2014) [arXiv:1402.2251 [hep-ph]].

[6] J. Herrero-Garcia, M. Nebot, N. Rius and A. Santamaria, Nucl. Phys. B **885**, 542 (2014) [arXiv:1402.4491 [hep-ph]].

[7] H. N. Long and V. V. Vien, Int. J. Mod. Phys. A **29**, no. 13, 1450072 (2014) [arXiv:1405.1622 [hep-ph]].

[8] V. Van Vien, H. N. Long and P. N. Thu, arXiv:1407.8286 [hep-ph].

[9] M. Aoki, S. Kanemura, T. Shindou and K. Yagyu, JHEP **1007**, 084 (2010) [Erratum-ibid. **1011**, 049 (2010)] [arXiv:1005.5159 [hep-ph]].

[10] M. Lindner, D. Schmidt and T. Schwetz, Phys. Lett. B **705**, 324 (2011) [arXiv:1105.4626 [hep-ph]].

[11] S. Baek, P. Ko, H. Okada and E. Senaha, JHEP **1409**, 153 (2014) [arXiv:1209.1685 [hep-ph]].

[12] M. Aoki, J. Kubo and H. Takano, Phys. Rev. D **87**, no. 11, 116001 (2013) [arXiv:1302.3936 [hep-ph]].

[13] Y. Kajiyama, H. Okada and K. Yagyu, Nucl. Phys. B **874**, 198 (2013) [arXiv:1303.3463 [hep-ph]].

[14] Y. Kajiyama, H. Okada and T. Toma, Phys. Rev. D **88**, 015029 (2013) [arXiv:1303.7356].

[15] S. Baek, H. Okada and T. Toma, JCAP **1406**, 027 (2014) [arXiv:1312.3761 [hep-ph]].

[16] H. Okada, arXiv:1404.0280 [hep-ph].

[17] H. Okada, T. Toma and K. Yagyu, Phys. Rev. D **90**, no. 9, 095005 (2014) [arXiv:1408.0961 [hep-ph]].

[18] H. Okada, arXiv:1503.04557 [hep-ph].

[19] C. Q. Geng and L. H. Tsai, arXiv:1503.06987 [hep-ph].

[20] S. Kashiwase, H. Okada, Y. Orikasa and T. Toma, Int. J. Mod. Phys. A **31**, no. 20n21, 1650121 (2016) doi:10.1142/S0217751X16501219 [arXiv:1505.04665 [hep-ph]].

[21] M. Aoki and T. Toma, JCAP **1409**, 016 (2014) [arXiv:1405.5870 [hep-ph]].

[22] S. Baek, H. Okada and T. Toma, Phys. Lett. B **732**, 85 (2014) [arXiv:1401.6921 [hep-ph]].

[23] H. Okada and Y. Orikasa, Phys. Rev. D **93**, no. 1, 013008 (2016) doi:10.1103/PhysRevD.93.013008 [arXiv:1509.04068 [hep-ph]].

[24] D. Aristizabal Sierra, A. Degee, L. Dorame and M. Hirsch, JHEP **1503**, 040 (2015) [arXiv:1411.7038 [hep-ph]].

[25] T. Nomura and H. Okada, Phys. Lett. B **756**, 295 (2016) [arXiv:1601.07339 [hep-ph]].

[26] T. Nomura, H. Okada and Y. Orikasa, arXiv:1602.08302 [hep-ph].

[27] C. Bonilla, E. Ma, E. Peinado and J. W. F. Valle, arXiv:1607.03931 [hep-ph].

[28] M. Kohda, H. Sugiyama and K. Tsumura, Phys. Lett. B **718**, 1436 (2013) [arXiv:1210.5622 [hep-ph]].

[29] B. Dasgupta, E. Ma and K. Tsumura, Phys. Rev. D **89**, 041702 (2014) [arXiv:1308.4138 [hep-ph]].

[30] S. Baek, JHEP **1508**, 023 (2015) doi:10.1007/JHEP08(2015)023 [arXiv:1410.1992 [hep-ph]].

[31] T. Nomura and H. Okada, Phys. Rev. D **94**, 075021 (2016) doi:10.1103/PhysRevD.94.075021 [arXiv:1607.04952 [hep-ph]].

[32] T. Nomura and H. Okada, arXiv:1609.01504 [hep-ph].

[33] T. Nomura, H. Okada and Y. Orikasa, Phys. Rev. D **94**, no. 11, 115018 (2016) doi:10.1103/PhysRevD.94.115018 [arXiv:1610.04729 [hep-ph]].

[34] Z. Liu and P. H. Gu, arXiv:1611.02094 [hep-ph].

[35] Y. F. Liang *et al.*, Phys. Rev. D **93**, no. 10, 103525 (2016) doi:10.1103/PhysRevD.93.103525 [arXiv:1602.06527 [astro-ph.HE]].

[36] R. J. Barlow, Nucl. Phys. Proc. Suppl. **218**, 44 (2011). doi:10.1016/j.nuclphysbps.2011.06.009

[37] E. Ma, Phys. Rev. D **73**, 077301 (2006) doi:10.1103/PhysRevD.73.077301 [hep-ph/0601225].

[38] Z. Maki, M. Nakagawa and S. Sakata, Prog. Theor. Phys. **28**, 870 (1962). doi:10.1143/PTP.28.870

[39] C. Guo, S. Y. Guo, Z. L. Han, B. Li and Y. Liao, arXiv:1701.02463 [hep-ph].

[40] D. V. Forero, M. Tortola and J. W. F. Valle, Phys. Rev. D **90**, no. 9, 093006 (2014) doi:10.1103/PhysRevD.90.093006 [arXiv:1405.7540 [hep-ph]].

[41] E. V. Hungerford [COMET Collaboration], AIP Conf. Proc. **1182**, 694 (2009).

[42] C. Dohmen *et al.* [SINDRUM II Collaboration], Phys. Lett. B **317**, 631 (1993).

[43] W. H. Bertl *et al.* [SINDRUM II Collaboration], Eur. Phys. J. C **47**, 337 (2006).

[44] W. Honecker *et al.* [SINDRUM II Collaboration], Phys. Rev. Lett. **76**, 200 (1996).

[45] K. Griest and D. Seckel, Phys. Rev. D **43**, 3191 (1991). doi:10.1103/PhysRevD.43.3191

[46] P. A. R. Ade *et al.* [Planck Collaboration], Astron. Astrophys. **571**, A16 (2014) doi:10.1051/0004-6361/201321591 [arXiv:1303.5076 [astro-ph.CO]].

[47] D. S. Akerib *et al.*, arXiv:1608.07648 [astro-ph.CO].

[48] R. Gastmans, S. L. Wu and T. T. Wu, arXiv:1108.5872 [hep-ph].

[49] L. Feng, Y. F. Liang, T. K. Dong and Y. Z. Fan, Phys. Rev. D **94**, no. 4, 043535 (2016) doi:10.1103/PhysRevD.94.043535 [arXiv:1608.04056 [hep-ph]].

[50] T. Hambye, K. Kannike, E. Ma and M. Raidal, Phys. Rev. D **75**, 095003 (2007) doi:10.1103/PhysRevD.75.095003 [hep-ph/0609228].

[51] S. Tulin, H. B. Yu and K. M. Zurek, Phys. Rev. D **87**, no. 11, 115007 (2013) doi:10.1103/PhysRevD.87.115007 [arXiv:1302.3898 [hep-ph]].